NANO LETTERS

2008
Vol. 8, No. 10
3418-3422

Electromechanical Unzipping of Individual DNA Molecules Using Synthetic Sub-2 nm Pores

Ben McNally, Meni Wanunu, and Amit Meller*

Department of Biomedical Engineering, Department of Physics, Boston University, Boston, Massachusetts

Received July 22, 2008; Revised Manuscript Received August 10, 2008

ABSTRACT

Nanopores have recently emerged as high-throughput tools for probing and manipulating nucleic acid secondary structure at the single-molecule level. While most studies to date have utilized protein pores embedded in lipid bilayers, solid-state nanopores offer many practical advantages which greatly expand the range of applications in life sciences and biotechnology. Using sub-2 nm solid-state nanopores, we show for the first time that the unzipping kinetics of individual DNA duplexes can be probed by analyzing the dwell-time distributions. We performed high-bandwidth electrical measurements of DNA duplex unzipping as a function of their length, sequence, and temperature. We find that our longer duplexes (>10 bp) follow Arrhenius dependence on temperature, suggesting that unzipping can be approximated as a single-barrier crossing, but the unzipping kinetics of shorter duplexes do not involve a barrier, due to the strong biasing electrical force. Finally, we show that mismatches in the duplex affect unzipping times in a position-sensitive manner. Our results are a crucial step toward sequence variability detection and our single-molecule nanopore sequencing technology, which rely on parallel detection from nanopore arrays.

Nanopores have recently emerged as simple and unique tools for the manipulation and analysis of biopolymers at the single-molecule level.[1−3] A nanopore device consists of a molecularly wide single pore through an impermeable membrane. Application of voltage across the membrane results in an ion-current signal, which transiently changes upon capture from solution of randomly diffusing biopolymers. Charged molecules, such as polynucleic acids, can be sequentially driven through the nanopore by the voltage-induced force. In addition to probing primary nucleic acid structure (length, sequence),[4−7] nanopores have been used to explore secondary structure by using the electrical force to unzip duplex regions.[8−13] The lipid-embedded α-hemolysin channel has been a model nanopore system for such experiments, although the fragility of the lipid bilayer and lateral diffusion of the channels in the membrane are major drawbacks that hinder prospective biotechnological nanopore applications. A more practical nanopore platform would ideally consist of a robust planar membrane design which contains nanopores at laterally specified positions, allowing the incorporation of complementary probing approaches, such as optical imaging and transverse electron tunneling, thus enabling high-throughput parallel detection from many pores.[14,15]

Recent developments in synthetic nanopore fabrication have enabled nanopores of tunable dimensions to be constructed in robust solid-state membranes.[14,16,17] Using either focused ion beams or electron beams, nanopores and nanopore arrays have been fabricated in ultrathin solid-state membranes, achieving subnanometer nanopore size accuracy. Solid-state nanopores with diameters between the ssDNA and dsDNA hydrodynamic cross-sections (i.e., 1.5−2 nm) are ideal candidates for determining the unzipping kinetics of DNA secondary structure, since shear force can be applied to induce DNA unzipping. A recent report has employed quantitative PCR (qPCR) to show that similar to protein pores, nanoscale synthetic pores can be used to electromechanically unzip DNA duplexes.[13] However, direct measurement of single-molecule unzipping kinetics through solid-state pores has yet to be reported.

In this letter, we employ high-bandwidth electrical measurements to investigate the unzipping kinetics of hybrid DNA structures containing duplex regions of different lengths and sequences. We show that individual unzipping events can be resolved and that subtle mismatches in the duplex region result in easily distinguishable, shorter timescales than the perfect complement. We also find that the position of the mismatch in the duplex region strongly affects unzipping timescales. A systematic temperature-dependence study of the unzipping kinetics reveals that the process can be well-approximated by first-order kinetics, similar to those reported for the α-hemolysin system.[8−10] Our findings demonstrate direct readout of individual unzipping events, circumventing

* To whom correspondence should be addressed. E-mail: ameller@bu.edu.

10.1021/nl802218f CCC: $40.75
Published on Web 08/30/2008

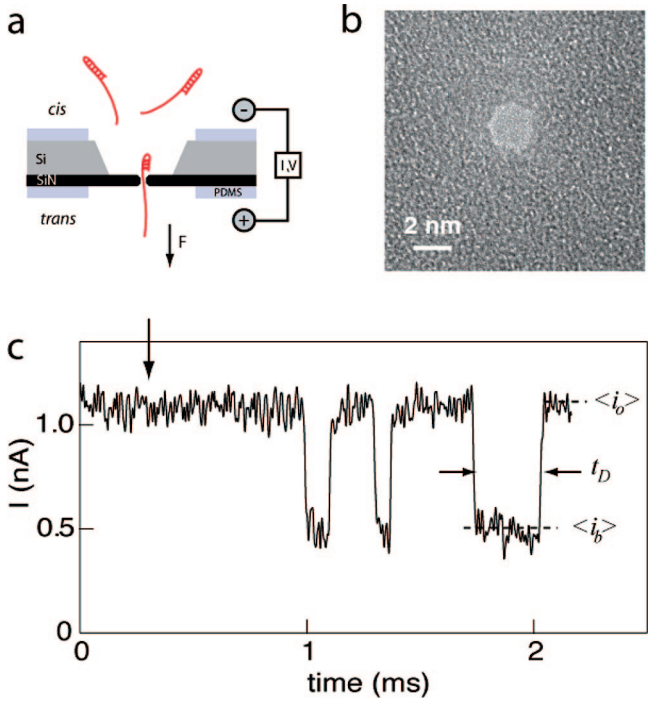

Figure 1. Solid-state nanopore device for unzipping DNA molecules. (a) Scheme of our setup, consisting of a 1.7−2.0 nm pore fabricated in an ultrathin SiN membrane. A voltage is applied across the membrane, and electrolyte flow through the pore provides the signal. Single-stranded DNA threading results in an applied force, which is used to unzip the duplex region in the molecule. (b) A top-view TEM image of a 2 nm pore fabricated by a TEM electron beam. (c) Current−time trace of a 2 nm pore at 300 mV applied voltage, before and after the addition of a 24-bp duplex (**HP24**, see Supporting Information) to the cis chamber, marked by an arrow. DNA entry is signaled by the downward spikes, with corresponding dwell-times t_D and current levels i_o and i_b, as shown in the figure (time between events was excised in order to better display the events).

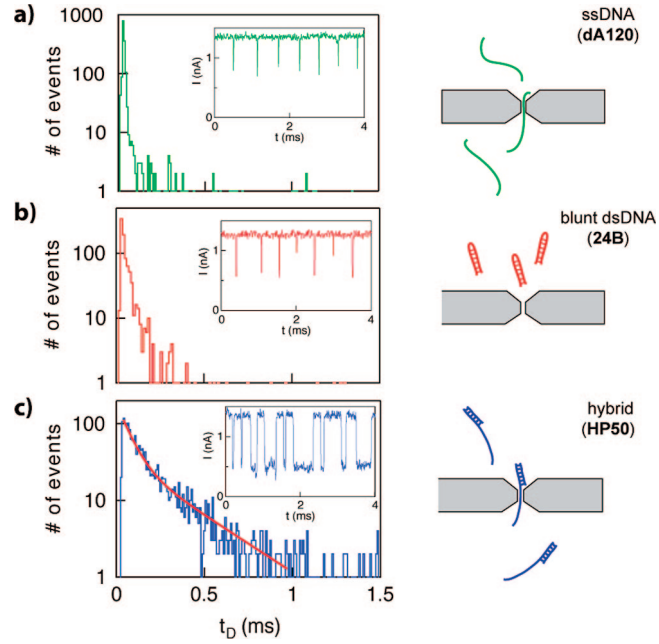

Figure 2. Dwell-time distributions for three DNA samples through 2 nm pores. (a) a ssDNA molecule consisting of 120-mer poly deoxyadenine molecule. (b) Blunt dsDNA, consisting of a 24-bp duplex region and a 6-base loop. (c) A hybrid single-strand/duplex molecule, consisting of a 100-mer strand hybridized to a fully complementary 50-mer at one end. While the dwell-times for ssDNA and blunt dsDNA are short (<21 μs), noticeably longer dwell-times are observed for the hybrid molecule. The complete dwell-time distribution for the hybrid molecule can be modeled as a biexponential function with decay timescales $t_0 = 40$ μs and $t_1 = 240$ μs, corresponding to a collision and translocation/unzipping process, respectively. Typical events for the three samples are shown as insets to the dwell-time distributions.

the need for time-consuming PCR amplification. These features pave the way for nanopore-based single nucleoide polymorphism detection, further constituting a key component in the development of our high-throughput DNA sequencing method.[15]

DNA oligonucleotides were purchased from Eurogentec (Eurogentec, San Diego, CA) and purified by either PAGE or HPLC. Prior to each experiment, hairpin molecules were heated to 95 °C in a temperature bath and then quickly cooled on ice. DNA hybrids were prepared by heating complementary strands to 95 °C and followed by slow cooling using a thermal cycler. To verify proper hybridization, nondenaturing PAGE was performed on each DNA product. The structures of the molecules used in this paper are provided in the Supporting Information. Solid-state nanopores were fabricated using an electron beam as described earlier, and electrical recordings from single nanopores were carried out using a custom cell design as described in ref 3 (see Supporting Information for details).

Figure 1a displays schematically a profile of our solid-state nanopore setup for unzipping DNA molecules (not to scale). A TEM top view image of a portion of the SiN membrane containing a 2 nm pore is shown in Figure 1b.

For all the nanopores used in this study, we found linear $I-V$ curves with conductance values 3−4.5 nS, and an open pore current value which remained unchanged over hours of measurement. The effective diameter of our nanopores was found to be 1.7−2.0 nm, based on analysis of the TEM images and the conductance values.[14] Upon addition of hairpin DNA molecules into the cis chamber and the application of 300 mV to the trans chamber (arrow in Figure 1c), we observe distinct, stochastic current blockade events, corresponding to single molecules dwelling in the pore. With each entry of a DNA molecule to the pore, the ion current is reduced from ~1.1 nA (the open pore current, or $\langle i_o \rangle$) to ~0.5 nA (the blocked current level, or $\langle i_b \rangle$, with an event duration (or dwell-time) of t_D). Statistically meaningful information was obtained by analysis of thousands of dwell-time events for each DNA sample and experimental conditions.

To pull a duplex DNA molecule into a sub-2 nm pore, a single-stranded overhang is required. To illustrate this, we compare in Figure 2 the dwell-time distributions for three different molecules: (a) an unstructured ssDNA 120-mer deoxyadenine homopolymer (**dA120**). (b) A blunt-ended DNA hairpin molecule consisting of a 24 bp stem (**24B**). (c) A DNA hybrid with a 50 bp duplex region and a 50-mer single-stranded overhang (**HP50**). Typical translocation events and dwell-time distributions are shown in Figure

2a−c, respectively. The single-stranded polymer (**dA120**) exhibits extremely short dwell-times with a peak at ~24 μs, followed by an exponential decay with $\tau = 8.8 \pm 0.4$ μs. Similarly, we find for the blunt-ended hairpin (**24B**) a peak at 24 μs, followed by a decay with time scale $\tau = 21.1 \pm 1.2$ μs. In contrast, **HP50** produces much longer dwell-times, characterized by a peak at ~40 μs and a broad biexponential decay with characteristic timescales $t_0 = 40 \pm 6$ μs and $t_1 = 240 \pm 22$ μs. Two timescales were previously observed with α-hemolysin with the fast time scale (t_0) being attributed to collisions and the slower (t_1) to translocation (or unzipping).[4] While **HP50** is merely a fusion of ssDNA to blunt dsDNA, the appearance of a much longer time scale (t_1) as compared to either of the two separate components, suggests that this molecule undergoes a different process when threaded through the nanopore.

Upon threading of the single-stranded portion, the duplex portion encounters the <2 nm constriction of the pore. At this stage, the molecule can (1) retract backward to the cis chamber, (2) translocate through the nanopore with the duplex region intact (i.e., without unzipping), (3) unzip, as the shear force applied to the overhang strand breaks the duplex. Retraction of the DNA against the strong applied electrostatic force (option 1) is highly unlikely, as the probability of a unit charge thermally moving against the 300 mV potential[18] is $e^{-eV/k_BT} \sim e^{-11}$. Moreover, a backward retraction of the ssDNA overhang from the pore would be insensitive to the duplex region's length or its sequence. As we show later, t_1 strongly depends on the duplex properties, (length and sequence), clearly ruling out option 1. Option 2 is also improbable, since the diameters of the nanopores used in these experiments are smaller than the 2.2 nm duplex DNA cross-section. However, the data shown in Figure 2 is insufficient to unambiguously rule out option 2, since the DNA duplex may squeeze through the pore in a highly compressed conformation.[19]

We note that translocation of duplex DNA through <2 nm pores (option 2) is not expected to be sensitive to subtle sequence mismatches in the duplex region, which in contrast is expected to strongly affect the unzipping kinetics of the duplex. In Figure 3, we compare the dwell-time distributions for a 24 bp duplex region containing either a perfect complement (**PC**), or an identical sequence containing two consecutive purine-purine mismatches (**2MM**) in the middle of the duplex region. We note that under our experimental conditions, both structures are thermodynamically stable and duplex hybridization was confirmed using PAGE (inset) with both samples showing similar migration rates. Despite this, we observed strikingly distinguishable dwell-time dynamics for the two samples: while t_0 values were similar (60 ± 5 μs), we found that the t_1 time scale of **PC** (690 ± 85 μs) is twice as long as the corresponding t_1 value for **2MM** (320 ± 20 μs). In the context of option 2, that is, translocation of a deformed duplex portion without unzipping, we expect these molecules to display similar translocation timescales, as both have identical lengths. Moreover, we would expect that the two pairs of bulkier purines (GG/AA) in the middle of the **2MM** duplex would further slow down translocation

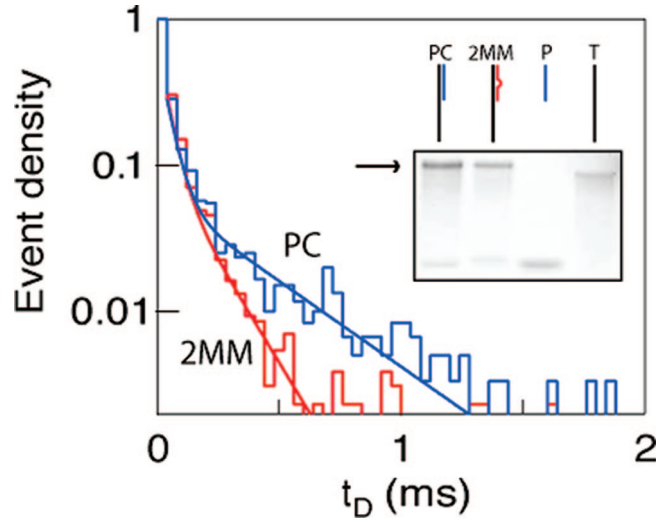

Figure 3. Dwell-time distributions for two hybrid molecules differing in their degree of complementarity (collected for a 2 nm pore at 0 °C, 300 mV). The template (**T**) is a 74-base ssDNA, to which one of two primers have been hybridized at one end. For **PC**, the 24-mer is a perfect complement, while for **2MM**, the 24-mer contains two adjacent purine/purine mismatches in the middle of the sequence. The t_1 time scale for **2MM** is twice as fast as that for **PC**. **PC** and **2MM** display nearly identical motilities on a nondenaturing PAGE (inset).

if the duplex were to transverse the pore, as compared with the **PC** molecule. Our results clearly show the opposite trend from which we can rule out option 2, concluding that t_1 represents the unzipping time of the duplex. This leads to a number of experimentally testable predictions, as discussed below.

Recent studies using α-hemolysin have demonstrated that DNA unzipping follows single-barrier activation process,[8−10] empirically described by the Kramers' rate model, $t_U = Ae^{((\Delta G^+ - qV)/k_BT)}$, where ΔG^+ is the activation energy for unzipping of the duplex, qV is the work done by the applied field, a product of the effective charge of the DNA strand in the pore (q) and the applied voltage (V), and A is the reciprocal of the unzipping attempt rate. To evaluate the validity of the Kramers' model in solid-state nanopores, we have explored the dependence of the dwell-time distributions on temperature, ranging from 0 to 21 °C for different length of duplexes ($N = 5$, 10, 16, and 24). In all cases, the dwell-time distributions (>2000 events for each case) closely resemble the biexponential form showed in Figure 3. Figure 4 displays the dependence of t_1 on $1/T$ for all lengths measured. Error bars in the plot represent the uncertainty in t_1 determination obtained from the reduced χ^2 fits to the dwell-time distributions. For our longer duplexes ($N = 16$ and 24) we observe clear Arrhenius dependence (lines) indicating an activated process, while for the shorter duplexes much less pronounced temperature dependence is observed (dashed lines show linear fits to $1/T$).

To rationalize these observations we evaluate the reduction in the terminal unfolded state energy due to the electrical force. In accordance with previous publications, we estimate the upper limit of the electrical work done during unzipping

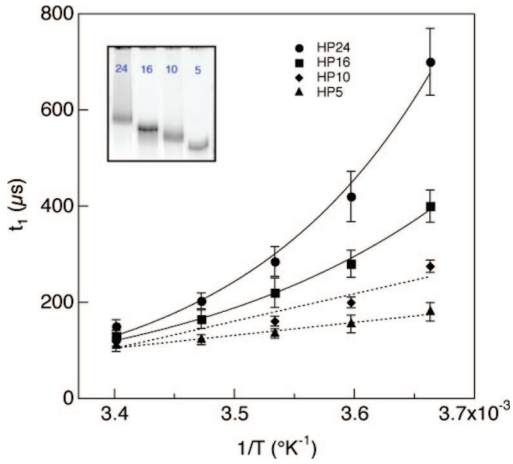

Figure 4. Unzipping times extracted from the dwell-time distributions, as a function of temperature for duplexes in the range 5−24 bp. Solid lines represent Arrhenius fits and dashed lines are linear approximations to the data. The inset displays a PAGE of the four hairpin molecules, stained using dsDNA stain SYBR Green I.

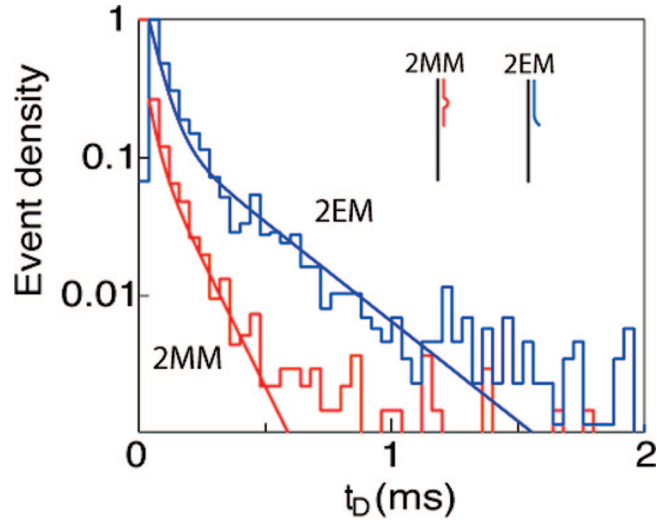

Figure 5. The unzipping time is extremely sensitive to the position of a 2-base mismatch in the duplex region. A comparison of the dwell-time distributions for two hybrid molecules differing only in the position of a 2-base mismatch: **2MM** is a hybrid of a 74-base template to a 24-mer oligonucleotide with two middle mismatches, and **2EM** contains two adjacent mismatches at the end of the sequence. While the t_1 time scale for **2EM** is practically indistinguishable from the perfect compliment (**PC**) shown in Figure 3, it is 2 times slower than the unzipping time of **2MM.** The data was collected for a 2 nm pore at 0 °C, 300 mV.

by $q_{\text{eff}}V$, with q_{eff} representing the total effective charge on the single-stranded overhang residing in the pore, to be in the range 20−80 k_BT.[10,20] Since we observe an apparent transition from a downhill unzipping to a thermally activated process between HP10 and HP16, we conclude that a lower limit for the electrical work lies in the range 23−42 k_BT, given the duplex free energies calculated using the Mfold server (http://mfold.bioinfo.rpi.edu). These values are within the expected electrical work applied in our experiments.

Another way to lower the activation energy is by introducing mismatches in stable duplex regions. As shown in Figure 2, introducing a 2-base mismatch in the middle of the 24-mer duplex effectively splits the unzipping process into two consecutive 11-mer steps. Given that we observed a transition in the unzipping kinetics between 10 and 16 bp (Figure 4), we expect to see a strong dependence on mismatch position: a middle mismatch would strongly shorten the unzipping time, whereas the same mismatch located at one of the ends would not. To confirm this idea, we performed unzipping experiments comparing the two-base mismatch 24-bp duplex (**2MM**) with an analogous duplex containing two adjacent mismatches at the end of the duplex (**2EM**), as shown in Figure 5. We find that **2EM** yields an unzipping time of $t_1 = 690 \pm 80$ μs (almost identical to the perfect compliment), in contrast to 320 ± 20 μs for **2MM**. This difference supports the idea that two-base middle mismatch forces the duplex to unzip in two consecutive downhill steps, each corresponding to ∼11 bp.

In conclusion, we have demonstrated that sub-2 nm solid-state nanopores can be used to unzip individual DNA molecules, and that the unzipping time scale can be directly measured from the dwell-times of the molecule inside the nanopore. The construct for unzipping experiments is straightforward, involving application of a voltage-induced shear force to a duplex molecule via a single-stranded "handle" across a nanopore. Information regarding the unzipping activation energy can be obtained by analysis of the dwell-time distribution, which displays biexponential form, with a short collision time scale followed by a long unzipping time scale. We have confirmed that duplex molecules unzip in sub-2 nm pores by comparing similar duplexes with subtle changes in their degree of complementarity, revealing that unzipping timescales are longer for the perfect complement. Introduction of a two-base mismatch reduces the unzipping time in a position-sensitive manner: we observed a 2-fold decrease when the mismatch was located in the middle of a 24-bp duplex, whereas placing the mismatch at the end of the duplex region resulted in a nearly indistinguishable unzipping time from the perfect complement.

The temperature dependence studies reveal a transition from an activated to downhill unzipping process, when the duplex free energy is ∼20−40 k_BT within the range of our estimated electrical work. By lowering the electrical field intensity, work currently underway, we envision that the sensitivity to shorter duplexes can be greatly enhanced. Our studies have unambiguously demonstrated that solid-state nanopores can be used to unzip short DNA duplexes, and that the unzipping timescale is the rate-limiting step for DNA translocation through sub-2 nm pores. These results represent an important milestone toward the development of an enzyme-free, ultrafast DNA sequencing method, involving the sequential unzipping and optical readout of fluorogenic probes, as well as high throughput sequence variability detection using nanopores.

Acknowledgment. We thank Gautam V. Soni, Jason Sutin, and Alon Singer for fruitful discussions. We also acknowledge the Center for Nanoscale Systems (CNS) at Harvard University, as well as financial support from NIH award HG004128 and NSF award PHY-0646637.

Supporting Information Available: Structures of the molecules used in all experiments, materials and methods, and analysis of the response time of our electrical measurements. This material is available free of charge via the Internet at http://pubs.acs.org.

References

(1) Dekker, C. *Nat. Nanotechnol.* **2007**, *2*, 209–215.
(2) Healy, K. *Nanomedicine* **2007**, *2*, 459–481.
(3) Wanunu, M.; Meller, A. In *Single-Molecule Techniques: A Laboratory Manual*; Selvin, P., Ha, T. J., Eds.; Cold Spring Harbor Laboratory Press: New York, 2008; p 395−420..
(4) Kasianowicz, J. J.; Brandin, E.; Branton, D.; Deamer, D. W. *Proc. Natl. Acad. Sci. U.S.A.* **1996**, *93*, 13770–13773.
(5) Akeson, M.; Branton, D.; Kasianowicz, J.; Brandin, E.; Deamer, D *Biophys. J.* **1999**, *77*, 3227–33.
(6) Meller, A.; Nivon, L.; Brandin, E.; Golovchenko, J.; Branton, D. *Proc. Natl. Acad. Sci. U.S.A.* **2000**, *97*, 1079–1084.
(7) Meller, A.; Nivon, L.; Branton, D. *Phys. Rev. Lett.* **2001**, *86*, 3435–3438.
(8) Sauer-Budge, A. F.; Nyamwanda, J. A.; Lubensky, D. K.; Branton, D. *Phys. Rev. Lett.* **2003**, *90*, 238101.
(9) Mathe, J.; Visram, H.; Viasnoff, V.; Rabin, Y.; Meller, A. *Biophys. J.* **2004**, *87*, 3205–3212.
(10) Mathe, J.; Arinstein, A.; Rabin, Y.; Meller, A. *Europhys. Lett.* **2006**, *73*, 128–134.
(11) Dudko, O.; Mathé, J.; Szabo, A.; Meller, A.; Hummer, G *Biophys. J.* **2007**, *92*, 4188–4195.
(12) Nakane, J.; Wiggin, M.; Marziali, A. *Biophys. J.* **2004**, *87*, 615–621.
(13) Zhao, Q.; Comer, J.; Dimitrov, V.; Yemenicioglu, S.; Aksimentiev, A.; Timp, G. *Nucleic Acids Res.* **2008**, *36*, 1532–1541.
(14) Kim, M. J.; Wanunu, M.; Bell, D. C.; Meller, A. *Adv. Mater.* **2006**, *18*, 3149–3153.
(15) Soni, G. V.; Meller, A. *Clin. Chem.* **2007**, *53*, 1996–2001.
(16) Li, J.; Stein, D.; McMullan, C.; Branton, D.; Aziz, M. J.; Golovchenko, J. A. *Nature* **2001**, *412*, 166–169.
(17) Storm, A. J.; Chen, J. H.; Ling, X. S.; Zandbergen, H. W.; Dekker, C. *Nat. Mater.* **2003**, *2*, 537–540.
(18) Lubensky, D. K.; Nelson, D. R. *Biophys. J.* **1999**, *77*, 1824–38.
(19) Heng, J. B.; Aksimentiev, A.; Ho, C.; Marks, P.; Grinkova, Y. V.; Sligar, S.; Schulten, K.; Timp, G. *Biophys. J.* **2006**, *90*, 1098–1106.
(20) Zhang, J.; Shklovskii, B. I. *Phys. Rev. E* **2007**, *75*, 021906.

NL802218F